Desalination and Water Treatment
www.deswater.com
doi: 10.5004/dwt.2019.24772

171 (2019) 67–77
December

Comparative study between aeration rate and membrane modification effects on antifouling properties of cellulose acetate membrane in membrane bioreactor systems

Habib Etemadi[a,*], Mehdi Motamed[b,c], Reza Yegani[b,c,*]

[a]*Department of Polymer Science and Engineering, University of Bonab, Bonab, Iran, email: h_etemadi@bonabu.ac.ir*
[b]*Faculty of Chemical Engineering, Sahand University of Technology, Tabriz, Iran*
[c]*Membrane Technology Research Center, Sahand University of Technology, Tabriz, Iran, emails: ryegani@sut.ac.ir (R. Yegani), mhd.motamed@gmail.com (M. Motamed)*

Received 1 March 219; Accepted 9 August 2019

ABSTRACT

In this paper, membrane modification and aeration rate effects on antifouling properties of cellulose acetate (CA) membrane in membrane bioreactor (MBR) systems were examined and the obtained results were compared. In phase I and for membrane modification, zinc oxide (ZnO) nanoparticles, 0–0.75 wt.%, were embedded in CA membrane. In this phase, scanning electron microscopy and contact angle measurements were used to determine the surface properties of the membranes, and optimal nanocomposite membrane was used in MBR for filtration of activated sludge. In phase II, four levels of aeration rate with specific aeration demand per membrane area (SADm) of 1, 2, 3 and 4 $m^3/m^2 h$ was used to investigate the effect of aeration rate on CA membrane fouling. The obtained results showed that maximum improvement in hydrophilicity and porosity of CA membrane was observed at 0.5 wt.% loading of ZnO nanoparticles. Also, either low or high aeration rate had a negative influence on permeability and antifouling properties of CA membrane. Under very high aeration rate (SADm > 2 $m^3/m^2 h$), the floc and particle breakage occur which these small matters can penetration through the membrane pores and membrane pore blockage or irreversible fouling occurs. By increasing aeration rate, chemical oxygen demand removal was increased and decreased for CA membrane and activated sludge, respectively. Finally, it was observed that the influence of membrane modification on the improvement of antifouling properties of CA membrane was more than optimal aeration rate effect.

Keywords: Membrane bioreactor; Cellulose acetate; Antifouling properties; Aeration rate; Nanocomposite membrane

1. Introduction

The discharge of wastewater that consists of different compounds from various industries into the environment has increased concerns about the environmental pollution. On the other hand, due to the water scarcity in many regions around the world, it seems that wastewater treatment and reuse are necessary. Among the wastewater treatment methods and water reuse process, membrane bioreactor (MBR) technology is the most feasible and innovative powerful tools [1,2]. MBR combines membrane filtration and biological activated sludge process and it has a small footprint and high quality of effluent compared with other conventional wastewater treatment systems [3,4]. However, membrane fouling is the major problem impeding the widespread adoption of MBR to full-scale plants [5].

Various methods have been used to reduce membrane fouling, including operational conditions and membrane modification. Among operational conditions parameters,

* Corresponding authors.

aeration in MBR systems is the most cost demanding factor in terms of energy consumption [6]. In this case, many studies have focused on the effect of aeration rate on the membrane fouling in the MBR systems. Dalmau et al. [6] showed that below aeration rate of 1 m h^{-1}, membrane fouling was increased and the values of transmembrane pressure (TMP) were doubled. Other studies have also shown an approach to define optimal operating conditions with respect to aeration rates [7]. Howell et al. [8] concluded that severe membrane fouling occurs if the permeate flux is too high or the aeration rate is too low. At moderate fluxes in the near-critical flux region, membrane fouling due to a temporary increase in permeate flux can be controlled by increasing the aeration rate. Meng et al. [9] examined membrane fouling in submerged MBRs operated under different aeration intensities and concluded that aeration had a positive effect on cake layer removal, but pore blocking became severe as aeration intensity increased to 800 L/h. De Temmerman et al. [10] also reported that during high aeration intensity, the total membrane fouling rate measurements increased significantly. It was showed in the study by Prat and Ducoste [11] a low average characteristic velocity gradient (low aeration rate) results in larger floc sizes in the activated sludge tank, while, high aeration rate creates smaller flocs. In the latter case, this is likely to result in a thicker cake layer, gel layer and pore blocking resistance compared with the former case.

Among membrane modification methods, modification of membranes with inorganic nanoparticles; that is, nanocomposite membrane, has been extensively studied due to its simplicity and cost effectiveness [12]. In this case, various nanoparticles such as TiO_2 [5,13], multiwalled carbon nanotubes [14], graphene oxide [12], nanodiamond [15], Fe_3O_4 [1], SiO_2 [3] were used in order to improve the hydrophilicity and antifouling properties of membranes in the MBR systems.

In the present study, the effect of aeration rate and membrane modification on antifouling properties of cellulose acetate (CA) membrane in the MBR systems was examined, and the obtained results were compared with each strategy. CA widely used in membrane separation process due to its high hydrophilicity, high biocompatibility, non-toxic nature, good desalting, high potential flux and relatively low cost [16,17]. However, high biofouling tendency and biodegradability are disadvantages of CA membranes in MBR media, necessitating the modification of CA [18,19].

It is well known that zinc oxide (ZnO) nanoparticles are one of the most suitable materials for improvement of the hydrophilicity and antibacterial activity of membranes [20]. ZnO nanoparticles are low cost and have excellent antibacterial activity as well as it can easily absorb hydrophilic hydroxyl groups (–OH) [21–23]. Several researches have been reported on the incorporation of ZnO nanoparticles into different polymer matrix membranes, such as polyvinyl chloride (PVC) [24], polysulfone [25], polyether sulfone [21], polyvinylidene fluoride [26] and polyethylene (PE) [22]. Alsalhy et al. [24] developed a nanocomposite flat sheet membrane from PVC/ZnO via induced phase separation method for actual hospital wastewater treatment in MBR systems. They concluded that the thickness of the cake layer formed on the membrane surface was reduced with an increase in ZnO nanoparticles. Also, chemical oxygen demand (COD) removal efficiency of the MBR process was approximately similar for neat PVC and nanocomposite membranes.

Most of the previous literatures separately focused on the effect of aeration rate or membrane modification effect on antifouling properties of membrane in MBR systems. According to our knowledge, there is no report about comparison between membrane modification and aeration rate effects on antifouling properties of membrane in MBR systems, in order to find effective strategy.

Therefore, in this paper, we examined both strategies, that is, membrane modification and aeration rate effects, on antifouling properties of CA membrane in MBR systems to treat a real wastewater sample obtained from Daana Pharmaceutical Company of Iran. For this purpose, several structural and operational analyses were carried out to find effective method about improvement in antifouling properties of CA membrane in MBR systems.

2. Experimental

2.1. Materials

The CA polymer (M_n = 30,000 g/mol) was obtained from Sigma-Aldrich (Germany), and the N-N-dimethylformamide (DMF, 99.8%) solvent was supplied by Merck (Darmstadt, Germany). ZnO nanoparticles (particle size < 100 nm) were purchased from Sigma-Aldrich.

2.2. Preparation of membranes

Non-solvent induced phase separation method was applied to prepare pure CA and ZnO-embedded membranes. First, different amounts of ZnO nanoparticles (0, 0.25, 0.5 and 0.75 wt.%) were added into the DMF solvent with continuous vigorous stirring for 6 h to make ZnO nanoparticles disperse uniformly. For better dispersion of the ZnO in solvent, the solution was sonicated for 3 h using a bath ultrasonic (WOSON Company, China) at 50 kHz. Subsequently, 17.5 wt.% of CA was dissolved in the solution at 2,000 rpm for 6 h and ultrasonic was used for 1 h. Then, the casting solution was cast onto a glass plate with a 200 μm casting knife by using automatic casting machine (Coa Test, Taiwan). The fabricated membranes were immersed in fresh distilled water for 24 h to remove all the residual solvent.

Under high loading of ZnO nanoparticles; that is, higher than 0.75 wt.%, mechanical and hydrophilicity of membrane significantly decreased (data not shown). Therefore, 0–0.75 wt.% of ZnO nanoparticles were chosen for CA nanocomposite membrane preparation.

2.3. Characterization

The morphology of the membranes was characterized by FE-SEM (MIRA3 FEG-SEM, Tescan). FESEM device was equipped with dispersive X-ray analysis (EDX) detector to inspect the existence of ZnO nanoparticles in the membranes. The hydrophilicity of the membranes surface as a function of different contents of ZnO nanoparticles was evaluated based on the static water contact angle using contact angle goniometer (PGX, Thwing-Albert Instrument Co., Germany). Water content (WC) of membranes was determined according to its dry-wet weight. Pieces of different membrane samples were

immersed in DI water at room temperature for 24 h and the weight of the wetted membrane (W_{wet}) was measured after mopping it with a filter paper. The dry weight (W_{dry}) was determined after 48 h drying at 75°C, the WC ratio was calculated by the following equation [27]:

$$WC\% = \frac{W_{wet} - W_{dry}}{W_{wet}} \times 100 \quad (1)$$

The porosity of the different membranes was calculated using Eq. (2) [28] as follows:

$$\varepsilon(\%) = \frac{(W_{wet} - W_{dry}) / D_w}{(W_{wet} - W_{dry}) / D_w + W_{dry} / D_p} \times 100 \quad (2)$$

where ε is the porosity of membrane (%), D_w (0.998 g/cm^3) and D_p (1.3 g/cm^3) are the density of the water and polymer, respectively.

The mean pore radius (r_m) was calculated based on water flux measurements using the Guerout–Elford–Ferry equation (Eq. (3)) [29]:

$$r_m = \sqrt{\frac{8\eta l Q(2.9 - 1.75\varepsilon)}{\varepsilon A \Delta P}} \quad (3)$$

where ΔP is trans-membrane pressure (TMP, Pa), A is the effective membrane area (m^2), ε is membrane overall porosity, Q is the volume of permeated pure water per unit time (m^{3}s^{-1}), η is the water viscosity (8.9 × 10^{-4} Pas), and l is the membrane thickness (m).

The tortuosity (τ) of the membrane was determined using Eq. (4) [30]:

$$\tau = \frac{(2 - \varepsilon)^2}{\varepsilon} \quad (4)$$

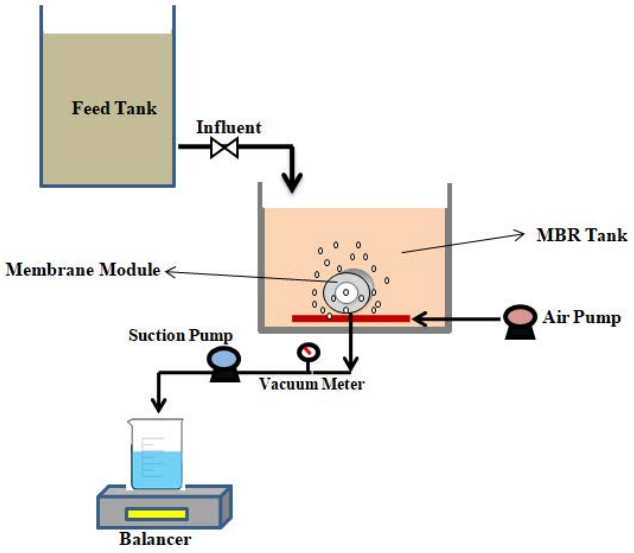

Fig. 1. Schematic of MBR setup in this study.

2.4. MBR apparatus and operational conditions

The schematic of the experimental setup was shown in Fig. 1. The reactor had a working volume of 12 L for the mixed liquor. The flat sheet membrane modules had a volume of 50 mL and an effective membrane filtration area of 14.7 cm^2. A porous air diffuser under the membrane module provided continuous aeration to create a shear force to hinder deposition of activated sludge particles on the membrane surface. TMP was maintained constant at 0.1 bar. Hydraulic retention time and sludge residence time were maintained at 24 h and 25 d, respectively. Mixed liquor suspended solids was controlled between 6,500 and 7,000 mg L^{-1}.

Real municipal wastewater with COD of 2,800 mg/L was supplied from plant of Daana Pharmaceutical Company of Tabriz, Iran. The experiment was divided into two phases. Phase I was carried out in order to determine the membrane modification effect on membrane fouling with specific aeration demand per membrane area (SADm) of 1 m^3/h m^2, and in this case, both pure CA and CA/ZnO nanocomposite membranes were used. Literature showed that air injection reduced fouling in a submerged MBR up to a critical flow rate corresponding to a SADm of 0.25 m^3/h m^2 [31,32]. In other words, beyond this value, increasing air flow did not have a positive effect on membrane fouling. Therefore, in this study, the SADm was corresponding to 1 m^3/h m^2. In phase II, the effect of aeration rate on CA membrane fouling was examined, and in this case, SADm was selected in four rates; 1, 2, 3 and 4 m^3/h m^2.

2.5. Analysis of membrane fouling

After pure water flux tests (J_{w1}, L/m^2 h), the flux for activated sludge (J_{AS}, L/m^2 h) was measured based on the water quantity permeating the membranes at 0.1 bar for 6 h. After filtration of activated sludge, the membranes were washed with distilled water, then the pure water flux of cleaned membranes J_{w2} (L/m^2 h) was measured again. The flux recovery ratio (FRR) was calculated as follows:

$$\mathrm{FRR}(\%) = \frac{J_{w2}}{J_{w1}} \times 100 \quad (5)$$

Generally, higher FRR indicates better antifouling property of the membranes [29].

The total fouling ratio (TFR), reversible fouling ratio (RFR) and irreversible fouling ratio (IFR) were calculated by using Eqs. (6)–(8) [15]:

$$\mathrm{RFR}(\%) = \left(\frac{J_{w2} - J_{AS}}{J_{w1}}\right) \times 100 \quad (6)$$

$$\mathrm{IFR}(\%) = \left(\frac{J_{w1} - J_{w2}}{J_{w1}}\right) \times 100 \quad (7)$$

$$\mathrm{TFR}(\%) = \mathrm{RFR}(\%) + \mathrm{IFR}(\%) = \left(\frac{J_{w1} - J_{AS}}{J_{w1}}\right) \times 100 \quad (8)$$

The quality of permeate water produced by the MBR process was analyzed. COD was determined by absorbance method (BioQuest CE2501). COD removal for membranes and activated sludge was estimated by measuring COD of effluent (COD_E) and influent (COD_I) and using the following equation:

$$\text{COD Removal}\ (\%) = \left(1 - \frac{COD_E}{COD_I}\right) \times 100 \quad (9)$$

3. Results and discussions

3.1. Hydrophilicity, porosity, water content and mean pore radius of membranes

The hydrophilicity of membrane surface can be analyzed by water contact angle measurement. The contact angles of the surfaces of pure CA and nanocomposite membranes are shown in Table 1. The contact angles of the nanocomposite membranes decreased as the amount of ZnO nanoparticles was increased up to 0.5 wt.%. A lower water contact angle means a higher hydrophilicity, indicating that the addition of ZnO nanoparticles enhanced the hydrophilicity of the membranes. Decrease in the interface energy of the nanocomposite membranes affected by the polar characteristics of ZnO nanoparticles, responsible for improvement in the hydrophilicity [31]. It should be noted that at ZnO loadings higher than 0.5 wt.% the contact angle increases. The possible reason for any increase in the water contact angle at high loading of nanoparticles, was that the agglomeration of the nanoparticles on the membrane surface [32], and consequently reduction occurred in the effective surface of the nanoparticles [21].

The porosity of membranes has been measured using gravimetric method and the results are shown in Table 1. It can be seen that the increasing in the concentration of ZnO nanoparticle increases membrane porosity and attains its maximum value at the concentration of 0.5 wt.%. The hydrophilic ZnO nanoparticles would accelerate the membrane formation process by speeding up the exchange rate between solvent and non-solvent. However, at higher loading of ZnO nanoparticles, a compact organic–inorganic network structure results in the decrease of membrane porosity. This trend might be related to the increasing in viscosity of the casting solution. The increased viscosity supports the diffusion of solvent from the solution over the inside diffusion of non-solvent (water) into the cast film, resulting in a lower membrane porosity [33].

As shown in Table 1, it is observed that when the ZnO content was 0.5 wt.%, the bulk porosity increased in the range of 77.1% decreasing its pore tortuosity. High hydrophilic nature of ZnO in the CA matrix can be a reason for this phenomenon, which increased the solution thermodynamic instability in the phase inversion process and resulted in the formation of large pores on the membrane. Similar results were reported by Khalid et al. [30].

The effect of ZnO nanoparticles on the water content of CA membrane, is shown in Table 1. As reported in the table, the water content increased with the increase of ZnO nanoparticles loading up to 0.5 wt.%. At high loading of nanoparticles (0.75 wt.%), water content decreased. The decreased surface hydrophilicity and the lower porosity may be reasons for reduction in water content. A similar trend in the water content has been reported elsewhere [15,18].

Table 1 indicates that the mean pore size of membranes increased from 32 to 64 nm when the ZnO content increased from 0 to 0.5 wt.%. Increasing in the hydrophilicity and inter-penetration velocity of the water-solvent, are responsible for increasing in the mean pore size [26].

3.2. Membrane morphology

Fig. 2 shows scanning electron microscopy (SEM) images from cross-section of both pure CA and CA/ZnO (0.5 wt.%) nanocomposite membranes. It can be seen that in the presence of ZnO nanoparticles, the numbers and length of finger-like macropores increase. In fact, the presence of ZnO in the casting solution affects the phase inversion process and subsequently the membrane structure. In other words, hydrophilic ZnO accelerates solvent–nonsolvent exchange in the phase inversion process due to appropriate interaction between ZnO and water.

The SEM images of surface for selected membranes; pure CA and CA/ZnO (0.5 wt.%), are shown in Fig. 3. According to Fig. 3a, the smooth membrane surface is formed for pure CA membrane. Similar observations were observed by Lv et al. [34] and Arthanareeswaran et al. [35]. The surface SEM images for CA/ZnO (0.5 wt.%) membranes in Fig. 3b showed that nanocomposite membrane has rougher surfaces than that of ZnO-free membrane. The increased roughness may be the result of more active nodular surface and non active surface in the aqueous phase [36].

The EDX analysis was rather important for verifying the elements present in the membrane matrix, therefore CA/ZnO (0.5 wt.%) membrane was examined for the presence of the zinc components. These results are shown in Fig. 4. It can be seen that Zn element is evenly distributed on the membrane surface. These observations can be explained with reasonable accuracy with the help of nanoparticles incorporation mechanism during the phase inversion process.

Table 1
Water contact angles, %WC, porosity, mean pore radius, and tortuosity for pure CA and its nanocomposite membranes

Membrane type	Water contact angle (°)	Water content (%)	ε (%)	r_m (nm)	τ
CA	68	67.9	72.7	32	2.23
CA/ZnO (0.25 wt.%)	66	70	75	41	2.08
CA/ZnO (0.5 wt.%)	53	72	77.1	64	1.96
CA/ZnO (0.75 wt.%)	58	69.2	74	50	2.14

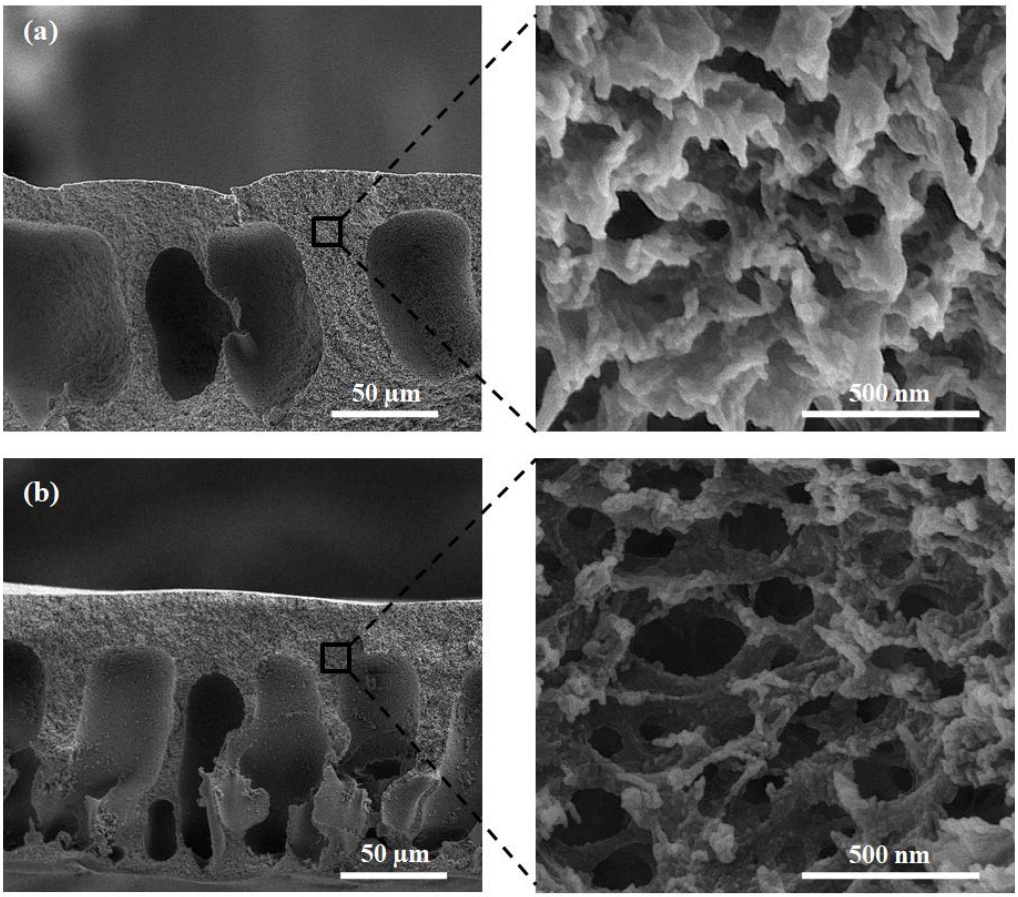

Fig. 2. FESEM images of cross section of membranes: (a) CA and (b) CA/ZnO (0.5 wt.%).

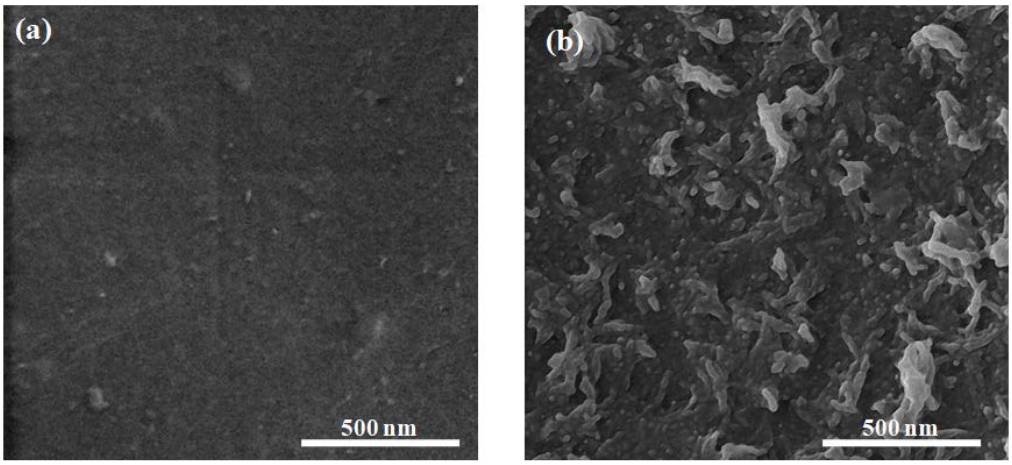

Fig. 3. FESEM images from top surface of membranes: (a) CA and (b) CA/ZnO (0.5 wt.%).

3.3. Fouling analysis and membrane performance

3.3.1. Effect of membrane modification

Evaluation of the fouling performance of the pure CA membrane and CA/ZnO (0.5 wt.%) nanocomposite membrane (modified membrane was selected among nanocomposite membranes) was carried out by using the pharmaceutical wastewater based on the flux decline during short-term activated sludge filtration (360 min) as depicted in Fig. 5. In this phase, the SADm was selected 1 m^3/m^2 h for both membranes (low aeration rate). The initial fluxes for unmodified and modified membranes were equal to 31.4 and 87.5 L/m^2 h, respectively. Although, the CA/ZnO (0.5 wt.%) membrane showed the maximum flux reduction through the filtration in a 6-h period, but at the end of filtration, nanocomposite membrane showed higher flux with respect to pure CA membrane.

It is well known that membrane fouling is considered as one of the main factors limiting the application of MBR. Generally, membrane fouling comprises reversible and irreversible fouling. If the foulants (such as colloidal particles, sludge flocs and cell debris) are weakly bound on the membrane surface or within its pores, reversible fouling occurs, which can be easily eliminated by water rinsing. While, irreversible fouling occurs, when the foulants are strongly attached within the pores or membrane surface and chemical cleaning is seriously needed to remove these foulants [29,37]. Fig. 6 shows values for FRR, TFR, reversible (RFR) and irreversible fouling ratio (IFR) were quantified during activated sludge filtration experiments. The initial pure water flux (J_{w1}) was measured 153 and 445 L/m^2 h for CA and CA nanocomposite membranes, respectively. Comparing the IFR values shows that incorporation of ZnO nanoparticles in CA matrix decreases irreversible fouling. Therefore, it seems that the presence of ZnO nanoparticles has a positive effect on the anti-fouling properties of CA membranes.

Higher values of FRR reflect lower persistent foulant adsorption to the membrane operated during the filtration. It can be seen in Fig. 6 that the FRR of nanocomposite membrane is higher than that of pure CA. The nanocomposite membrane displayed the FRR of 72%. The improved anti-fouling properties of modified membrane can be attributed to their improved hydrophilicity and microorganism repellency.

The SEM images in Fig. 7 exhibited the attached foulants (mainly bacteria) on the surface of both unmodified and modified membranes, that is, pure CA and CA/ZnO (0.5 wt.%), after physical washing. Obviously, the foulants which consist of bacteria or the mixed polymer aggregate with bacteria, were reduced significantly in CA/ZnO (0.5 wt.%) membrane compared with the pure membrane with a large colony of bacteria. In other words, the bacteria have strong interaction with pure CA membrane surface. It is well known that bacteria can attach on the both hydrophilic and hydrophobic surfaces, but it has been found that attachment of the bacteria to hydrophilic surfaces is the weaker of the hydrophobic surface [38]. Therefore, it is expected that after washing the membrane surface, nanocomposite membrane shows small colony of bacteria with respect to pure CA membrane. Also, many studies showed that ZnO nanoparticles possessed excellent antibacterial activity against various types of bacteria [33]. The antibacterial mechanism of ZnO nanoparticles could be due to damage to the membrane of bacterial cells by hydrogen peroxide or to the affinity between ZnO

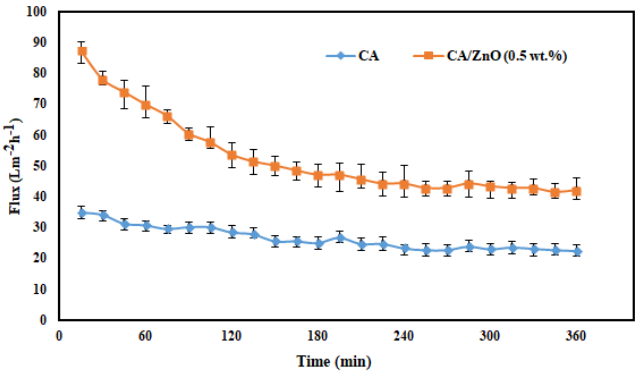

Fig. 5. Flux decline with operation time for pure CA and CA/ZnO (0.5 wt.%) membranes under conditions of constant SADm (1 m^3/m^2 h) and TMP (0.1 bar).

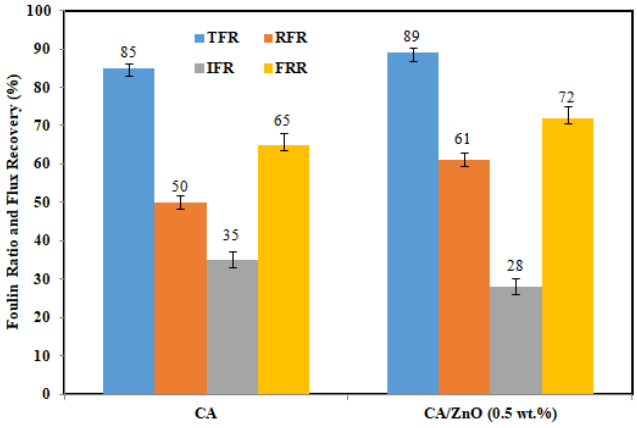

Fig. 6. Fouling parameters of both membranes during activated sludge filtration under conditions of constant SADm (1 m^3/m^2 h) and TMP (0.1 bar).

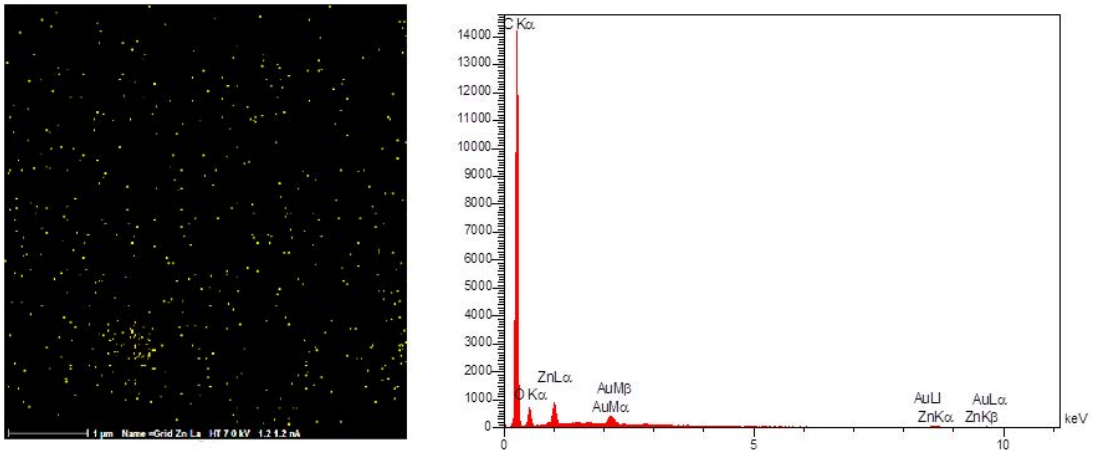

Fig. 4. EDX results of ZnO embedded CA membrane.

nanoparticles and bacterial which resulting in cell death [39]. However, due to the biodegradability of CA membranes, it is clear that the attached bacteria on the membrane surface can grow and damage the membrane. Therefore, ZnO nanoparticles can improve bacterial anti-adhesive properties as well as antibacterial activity of CA membranes.

3.3.2. Effect of aeration rate

In order to evaluate the effect of aeration rate on antifouling properties of CA membrane, the permeate flux is plotted against time in Fig. 8 for various SADm, that is, 1, 2, 3 and 4 m^3/m^2 h. As shown in Fig. 8, the membrane permeability at the end of filtration was decreased in the extreme low and high aeration rates. By increasing SADm from 1 to 2 m^3/m^2 h, the flux through the membrane increased at the whole of permeation time. At higher aeration rates, that is, 3 and 4 m^3/m^2 h, membrane permeability decreased. The results confirm the importance of aeration as a means to mitigate fouling in immersed membrane systems. However, there appears to be a practical limit above which the effect of increasing aeration has a minor added benefit.

The effect of aeration rate on fouling parameters of CA membrane is shown in Fig. 9. In the aeration rate of 2 m^3/m^2 h, CA membrane shows lowest IFR and TFR among other aeration rates. The IFR values were calculated to be 31% when the SADm increased from 1 to 2 m^3/m^2 h and were 64% when the SADm increased from 2 to 4 m^3/m^2 h. Also, values for FRR were 65%, 69%, 68% and 35% for SADm of 1, 2, 3 and 4 m^3/m^2 h, respectively.

Higher aeration rates more efficiently remove the fouling deposition or cake layer on the membrane surface due to the higher shear force of bubble air, and simultaneously increases the breakage of components that have been identified as major contributors to fouling. Fig. 10 shows the formation of cake layer on the membrane surfaces under the low and high aeration rates conditions. It is clear that more and thicker cake layer was formed on the membrane surface under the low aeration rate. Although, at low aeration rate, the formed biofilm layer was thicker, but loosely attached and can be easily removed physically [40].

Too high shear forces will have a detrimental effect on the suspended solids by breaking them up into smaller fragments. Breakage through aeration inevitably leads to higher concentrations of very small floc fragments in the bulk liquid. Fig. 11 shows the microscopic images of sludge flocs in mixed liquor under low (SADm = 1 m^3/m^2 h) and high (SADm = 4 m^3/m^2 h) aeration rates. According to Fig. 11, these images implied that the sludge floc mainly consisted of fiber-shape bacteria (filamentous bacteria). It is clear that a low aeration rate results in larger floc and particles sizes, while a higher aeration rate creates smaller particle and flocs due to the floc breakage [10,11].

These results showed that too high aeration intensity affected the sludge floc size and subsequently membrane

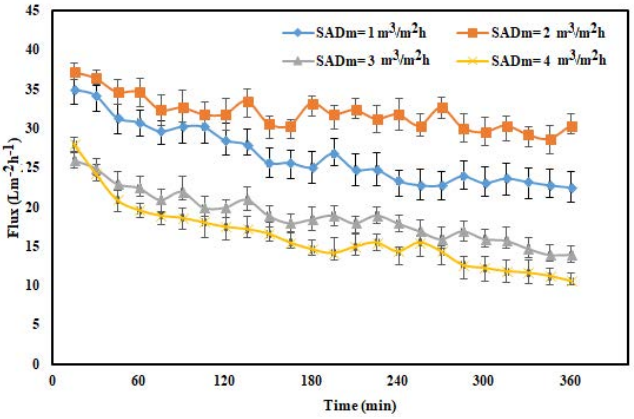

Fig. 8. Effect of aeration rate on the permeability of CA membrane in MBR system.

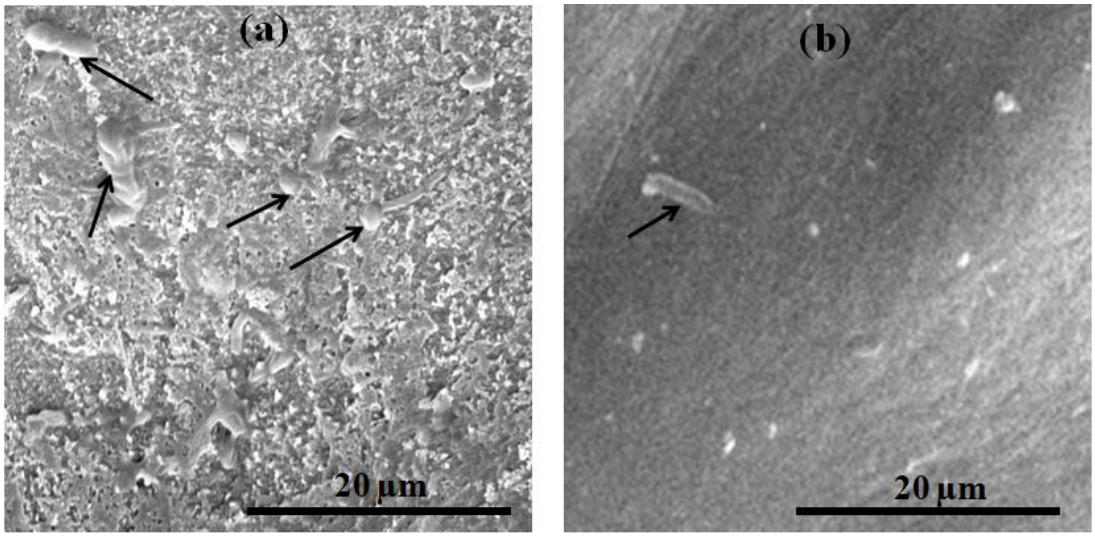

Fig. 7

Fig. 7. SEM images of attached foulants (mainly bacteria) on the washed membrane surfaces of (a) CA and (b) CA/ZnO (0.5 wt.%) after filtration of activated sludge.

fouling. This implies that the aeration rate largely determines the potential for floc breakage and release of small fragments into the bulk liquid which cause membrane pore blockage. As shown in Fig. 9, increase in aeration rate (higher than SADm of 2 m^3/m^2 h) results in irreversible fouling. The relation between aeration rate, flocculation behavior and membrane fouling is illustrated as schematically in Fig. 12. It can seen from Fig. 12a, under low aeration rate, due to larger size of sludge floc and other particles, these matters accumulated on the membrane surface and cake layer formed on the membrane surface which can easily remove physically or eliminated by water rinsing. However, under very high aeration rate (SADm > 2 m^3/m^2 h) the floc and particle breakage occurs which these small matters can penetrate through the membrane pores and membrane pore blockage or irreversible fouling occurs (Fig. 12b). According to the literature, it is reported that under high shear conditions in MBR, due to the breakage of microbial floc and colloidal particles which cause a rapid loss in membrane permeability [41,42].

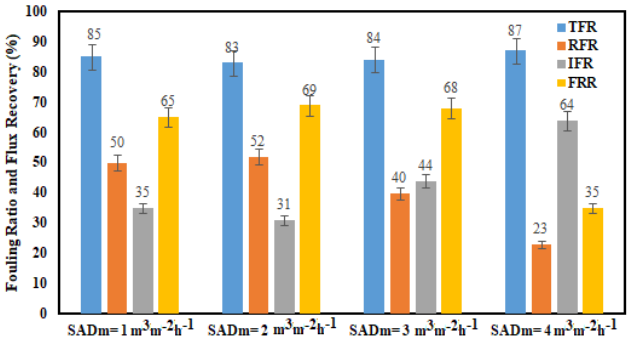

Fig. 9. Effect of aeration rate on fouling parameters of CA membrane.

Besides the aeration intensity and sludge floc size affected membrane fouling, it is expected that release of compounds such as soluble microbial products (SMP), which can be described as biopolymers, humic acids and the like, has been happened by floc breakage phenomena [43]. Literatures

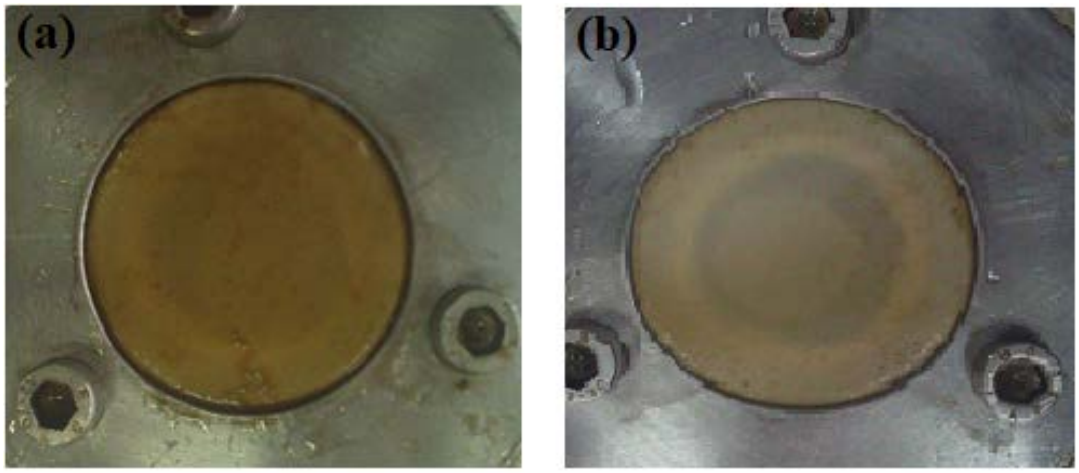

Fig. 10. Photograph of fouled CA membranes after MBR run under: (a) low (SADm = 1 m^3/m^2 h) and (b) high (SADm = 4 m^3/m^2 h) aeration rates.

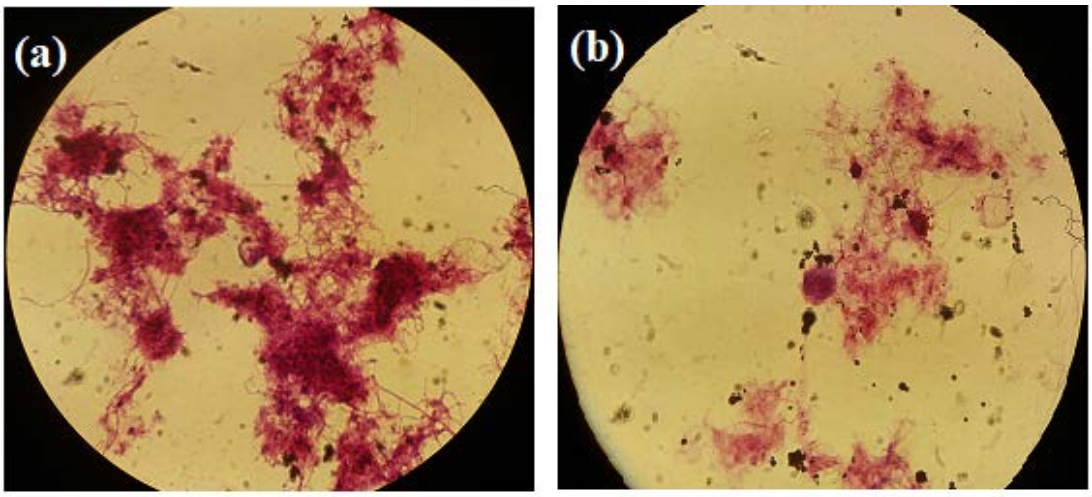

Fig. 11. Microscopic images of sludge flocs in mixed liquor under: (a) low (SADm = 1 m^3/m^2 h) and (b) high (SADm = 4 m^3/m^2 h) aeration rates.

showed that aeration intensity has some effect on biomass characteristics also since MBR system includes living microorganisms and their metabolites [6,10]. Also, it is well known that the adhesion and/or deposition of SMP toward membranes can block membrane pores and form a fouling layer, leading to an increase in the irreversible fouling and filtration resistance [15].

The effluent quality of the MBRs systems in terms of COD removal for both membrane and activated sludge at each aeration rate was shown in Fig. 13. The COD removal from activated sludge was primarily due to biological degradation in the bioreactor while COD removal in the permeate was due to simultaneous impact of membrane filtration and biofilm formation at low aeration rate (biofouling layer on the membrane surface) as well as pore blockage at high aeration rate. It is clear that COD removal for membrane was higher than activated sludge for difference aeration rates. Although the COD removal efficiency for membrane was excellent being more than 90% at any aeration rate, but by increasing aeration rate COD removal efficiency was decreased for activated sludge. According to the study be Meng et al. [9] and Temmerman et al. [10] studies, high aeration rates led to the release of SMP and breakage of particles and bacteria. Therefore, it is expected that COD removal efficiency of activated sludge was decreased by increasing aeration rates. This trend was observed elsewhere [41].

As shown in Fig. 13, the higher membrane COD removal was appeared at the highest aeration rate (SADm = 4 m^3/m^2 h). Similar trend of results was reported by Park et al. [41]. It could be concluded that high aeration rate results in breakage of particles and bacteria, and as mentioned previously, under high aeration rate membrane pore blockage occurs and particles and other foulants cannot cross through the membrane and therefore membrane COD removal increased.

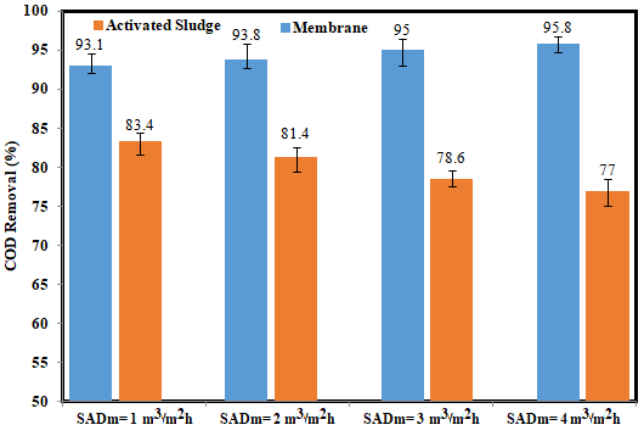

Fig. 13. Effect of aeration rate on the COD removal (%) of activated sludge and CA membrane permeation.

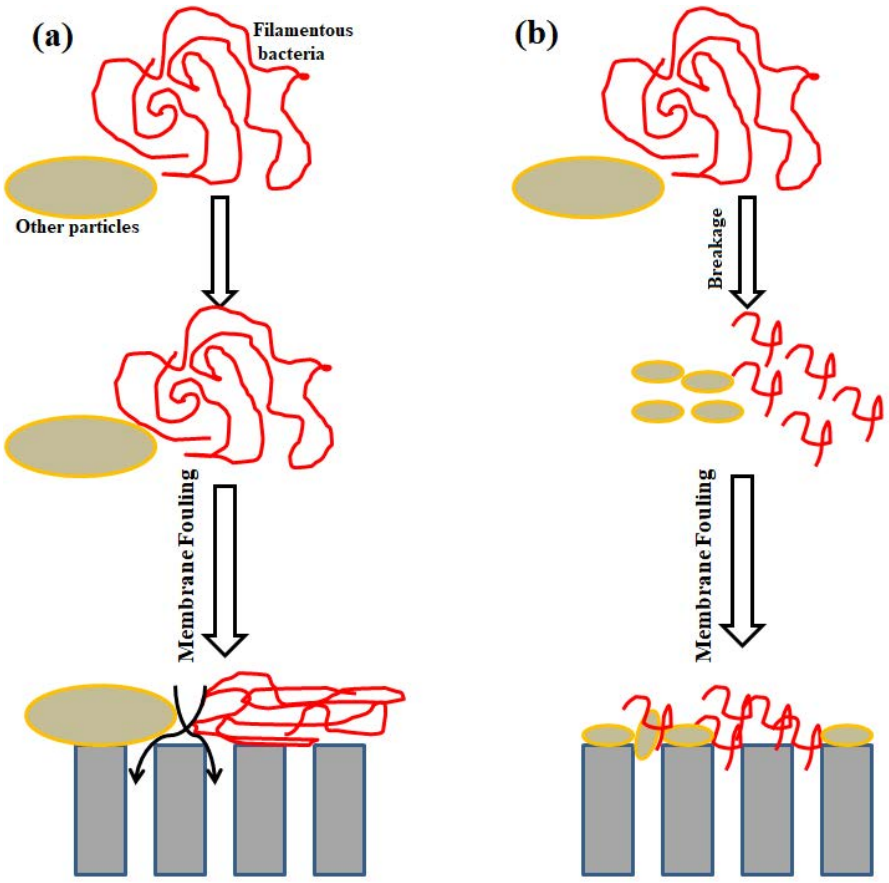

Fig. 12. Schematic of CA membrane fouling under: (a) low (SADm = 1 m^3/m^2 h) and (b) high (SADm = 4 m^3/m^2 h) aeration rates.

By comparing the obtained results from Figs. 6 and 9, it is clear that influence of membrane modification on the improvement of antifouling properties of CA membrane in MBR systems was more than aeration rate effect. The modified membrane or CA/ZnO (0.5 wt.%) nanocomposite membrane has lower IFR as well as higher FRR with respect to optimum aeration rate (SADm = 2 m^3/m^2 h). The main cost of total operation costs is due to aeration [44]. Therefore, although increasing in aeration rate up to optimum SADm membrane fouling decrease, but the cost of total operation can be increase. It is expected that the cost of modification membrane with low cost and effective nanoparticles such as ZnO is lower than the cost of increasing in aeration rate. On other hand, membrane modification is more effective in the improvement of antifouling properties of CA membrane in MBR with respect to aeration rate effect. However, it is important to note that these results and fouling parameters values are specific for the system and operating conditions applied in this study.

4. Conclusion

In this study, the impact of aeration rate as well as membrane modification on antifouling properties of CA membrane was comparatively examined in MBR systems. In order to achieve membrane modification, ZnO nanoparticles was embedded in CA membrane and its effect was examined in membrane fouling in MBR systems (phase I). Also, four levels of aeration rate with SADm of 1, 2, 3 and 4 m^3/m^2 h was used to investigate the effect of aeration rate on CA membrane fouling (phase II). Incorporation of 0.5 wt.% of ZnO resulted in the high values in the hydrophilicity, porosity and mean pore radios. The obtained results from phase I indicated that lower IFR and higher FRR for nanocomposite membrane confirm the advantages of the modified membrane. Although the significant reduction in the flux was observed for CA nanocomposite membrane, but the antifouling properties (such as lower IFR and higher FRR) for CA nanocomposite was more than pure CA membrane. According to the phase II, aeration intensity had significant impacts on membrane permeation. Low or high aeration rate had a negative influence on membrane permeability. Low aeration could not remove the membrane foulants from membrane surface effectively. However, high aeration could induce a severe breakage of sludge flocs. The SADm of 2 m^3/m^2 h was selected as optimal aeration rate, which low IFR and high RFR was occurred. Also, by increasing aeration rate, COD removal efficiency was increased and decreased for membrane and activated sludge, respectively. As a final result, it was concluded that the influence of membrane modification on the improvement in antifouling properties of CA membrane in MBR system was more than aeration rate effect.

References

[1] M.R. Mehrnia, M. Homayoonfal, Fouling mitigation behavior of magnetic responsive nanocomposite membranes in a magnetic membrane bioreactor, J. Membr. Sci., 520 (2016) 881–894.
[2] H.F. Zhang, H.P. Liu, L.H. Zhang, Applied research of nanocomposite membrane on fouling mitigation in membrane bioreactor, Advanced Materials Research, Trans. Tech. Publ., 2011, pp. 2019–2023.
[3] M. Amini, H. Etemadi, A. Akbarzadeh, R. Yegani, Preparation and performance evaluation of high-density polyethylene/silica nanocomposite membranes in membrane bioreactor system, Biochem. Eng. J., 127 (2017) 196–205.
[4] Q. Lei, F. Li, L. Shen, L. Yang, B.-Q. Liao, H. Lin, Tuning anti-adhesion ability of membrane for a membrane bioreactor by thermodynamic analysis, Bioresour. Technol., 216 (2016) 691–698.
[5] R.A. Damodar, S.-J. You, H.-H. Chou, Study the self cleaning, antibacterial and photocatalytic properties of TiO_2 entrapped PVDF membranes, J. Hazard. Mater., 172 (2009) 1321–1328.
[6] M. Dalmau, H. Monclús, S. Gabarrón, I. Rodriguez-Roda, J. Comas, Towards integrated operation of membrane bioreactors: effects of aeration on biological and filtration performance, Bioresour. Technol., 171 (2014) 103–112.
[7] I. Ivanovic, T. Leiknes, Impact of aeration rates on particle colloidal fraction in the biofilm membrane bioreactor (BF-MBR), Desalination, 231 (2008) 182–190.
[8] J. Howell, H. Chua, T. Arnot, In situ manipulation of critical flux in a submerged membrane bioreactor using variable aeration rates, and effects of membrane history, J. Membr. Sci., 242 (2004) 13–19.
[9] F. Meng, F. Yang, B. Shi, H. Zhang, A comprehensive study on membrane fouling in submerged membrane bioreactors operated under different aeration intensities, Sep. Purif. Technol., 59 (2008) 91–100.
[10] L. De Temmerman, T. Maere, H. Temmink, A. Zwijnenburg, I. Nopens, The effect of fine bubble aeration intensity on membrane bioreactor sludge characteristics and fouling, Water Res., 76 (2015) 99–109.
[11] O.P. Prat, J.J. Ducoste, Modeling spatial distribution of floc size in turbulent processes using the quadrature method of moment and computational fluid dynamics, Chem. Eng. Sci., 61 (2006) 75–86.
[12] C. Zhao, X. Xu, J. Chen, G. Wang, F. Yang, Highly effective antifouling performance of PVDF/graphene oxide composite membrane in membrane bioreactor (MBR) system, Desalination, 340 (2014) 59–66.
[13] T.-H. Bae, T.-M. Tak, Preparation of TiO_2 self-assembled polymeric nanocomposite membranes and examination of their fouling mitigation effects in a membrane bioreactor system, J. Membr. Sci., 266 (2005) 1–5.
[14] Z. Rahimi, A. Zinatizadeh, S. Zinadini, Preparation of high antibiofouling amino functionalized MWCNTs/PES nanocomposite ultrafiltration membrane for application in membrane bioreactor, J. Ind. Eng. Chem., 29 (2015) 366–374.
[15] H. Etemadi, R. Yegani, M. Seyfollahi, The effect of amino functionalized and polyethylene glycol grafted nanodiamond on anti-biofouling properties of cellulose acetate membrane in membrane bioreactor systems, Sep. Purif. Technol., 177 (2017) 350–362.
[16] H. Etemadi, R. Yegani, V. Babaeipour, Study on the reinforcing effect of nanodiamond particles on the mechanical, thermal and antibacterial properties of cellulose acetate membranes, Diam. Relat. Mater., 69 (2016) 166–176.
[17] H. Etemadi, R. Yegani, V. Babaeipour, Performance evaluation and antifouling analyses of cellulose acetate/nanodiamond nanocomposite membranes in water treatment, J. Appl. Polym. Sci., 134 (2017) 1–14.
[18] J. Dasgupta, S. Chakraborty, J. Sikder, R. Kumar, D. Pal, S. Curcio, E. Drioli, The effects of thermally stable titanium silicon oxide nanoparticles on structure and performance of cellulose acetate ultrafiltration membranes, Sep. Purif. Technol., 133 (2014) 55–68.
[19] J.-H. Choi, S. Dockko, K. Fukushi, K. Yamamoto, A novel application of a submerged nanofiltration membrane bioreactor (NF MBR) for wastewater treatment, Desalination, 146 (2002) 413–420.
[20] J. Hong, Y. He, Effects of nano sized zinc oxide on the performance of PVDF microfiltration membranes, Desalination, 302 (2012) 71–79.

[21] H. Rajabi, N. Ghaemi, S.S. Madaeni, P. Daraei, B. Astinchap, S. Zinadini, S.H. Razavizadeh, Nano-ZnO embedded mixed matrix polyethersulfone (PES) membrane: Influence of nanofiller shape on characterization and fouling resistance, *Appl. Surf. Sci*., 349 (2015) 66–77.
[22] Y. Jafarzadeh, R. Yegani, Thermal, mechanical, and structural properties of ZnO/polyethylene membranes made by thermally induced phase separation method, J. Appl. Polym. Sci., 132 (2015) 1–7.
[23] R.R. Darabi, M. Jahanshahi, M. Peyravi, A support assisted by photocatalytic Fe3O4/ZnO nanocomposite for thin-film forward osmosis membrane, Chem. Eng. Res. Des., 133 (2018) 11–25.
[24] Q.F. Alsalhy, F.H. Al-Ani, A.E. Al-Najar, S.I. Jabuk, A study of the effect of embedding ZnO-NPs on PVC membrane performance use in actual hospital wastewater treatment by membrane bioreactor, Chem. Eng. Process., 130 (2018) 262–274.
[25] C. Leo, W.C. Lee, A. Ahmad, A.W. Mohammad, Polysulfone membranes blended with ZnO nanoparticles for reducing fouling by oleic acid, Sep. Purif. Technol., 89 (2012) 51–56.
[26] J. Hong, Y. He, Polyvinylidene fluoride ultrafiltration membrane blended with nano-ZnO particle for photo-catalysis self-cleaning, Desalination, 332 (2014) 67–75.
[27] M. Sivakumar, A. Mohanasundaram, D. Mohan, K. Balu, R. Rangarajan, Modification of cellulose acetate: Its characterization and application as an ultrafiltration membrane, J. Appl. Polym. Sci., 67 (1998) 1939–1946.
[28] M. Zhang, R.W. Field, K. Zhang, Biogenic silver nanocomposite polyethersulfone UF membranes with antifouling properties, J. Membr. Sci., 471 (2014) 274–284.
[29] V. Vatanpour, S.S. Madaeni, A.R. Khataee, E. Salehi, S. Zinadini, H.A. Monfared, TiO_2 embedded mixed matrix PES nanocomposite membranes: Influence of different sizes and types of nanoparticles on antifouling and performance, Desalination, 292 (2012) 19–29.
[30] A. Khalid, A. Abdel-Karim, M.A. Atieh, S. Javed, G. McKay, PEG-CNTs nanocomposite PSU membranes for wastewater treatment by membrane bioreactor, Sep. Purif. Technol., 190 (2018) 165–176.
[31] A. Ding, H. Liang, G. Li, N. Derlon, I. Szivak, E. Morgenroth, W. Pronk, Impact of aeration shear stress on permeate flux and fouling layer properties in a low pressure membrane bioreactor for the treatment of grey water, J. Membr. Sci., 510 (2016) 382–390.
[32] T. Ueda, K. Hata, Y. Kikuoka, O. Seino, Effects of aeration on suction pressure in a submerged membrane bioreactor, Water Res., 31 (1997) 489–494.
[33] G.R. Guillen, Y. Pan, M. Li, E.M. Hoek, Preparation and characterization of membranes formed by nonsolvent induced phase separation: a review, Ind. Eng. Chem. Res., 50 (2011) 3798–3817.
[34] C. Lv, Y. Su, Y. Wang, X. Ma, Q. Sun, Z. Jiang, Enhanced permeation performance of cellulose acetate ultrafiltration membrane by incorporation of Pluronic F127, J. Membr. Sci., 294 (2007) 68–74.
[35] G. Arthanareeswaran, T.S. Devi, M. Raajenthiren, Effect of silica particles on cellulose acetate blend ultrafiltration membranes: Part I, Sep. Purif. Technol., 64 (2008) 38–47.
[36] H. Wu, B. Tang, P. Wu, Optimization, characterization and nanofiltration properties test of MWNTs/polyester thin film nanocomposite membrane, J. Membr. Sci., 428 (2013) 425–433.
[37] A. Behboudi, Y. Jafarzadeh, R. Yegani, Preparation and characterization of TiO_2 embedded PVC ultrafiltration membranes, Chem. Eng. Res. Des., 114 (2016) 96–107.
[38] M. Morra, C. Cassinelli, Bacterial adhesion to polymer surfaces: a critical review of surface thermodynamic approaches, J. Biomater. Sci., Polym. Ed., 9 (1998) 55–74.
[39] A. Sirelkhatim, S. Mahmud, A. Seeni, N.H.M. Kaus, L.C. Ann, S.K.M. Bakhori, H. Hasan, D. Mohamad, Review on zinc oxide nanoparticles: antibacterial activity and toxicity mechanism, Nano-Micro Letters, 7 (2015) 219–242.
[40] H. Choi, K. Zhang, D.D. Dionysiou, D.B. Oerther, G.A. Sorial, Effect of permeate flux and tangential flow on membrane fouling for wastewater treatment, Sep. Purif. Technol., 45 (2005) 68–78.
[41] J.-S. Park, K.-M. Yeon, C.-H. Lee, Hydrodynamics and microbial physiology affecting performance of a new MBR, membrane-coupled high-performance compact reactor, Desalination, 172 (2005) 181–188.
[42] J.-S. Kim, C.-H. Lee, I.-S. Chang, Effect of pump shear on the performance of a crossflow membrane bioreactor, Water Res., 35 (2001) 2137–2144.
[43] L. De Temmerman, T. Maere, H. Temmink, A. Zwijnenburg, I. Nopens, Salt stress in a membrane bioreactor: dynamics of sludge properties, membrane fouling and remediation through powdered activated carbon dosing, Water Res., 63 (2014) 112–124.
[44] P. Krzeminski, J.H. van der Graaf, J.B. van Lier, Specific energy consumption of membrane bioreactor (MBR) for sewage treatment, Water Sci. Technol., 65 (2012) 380–392.